IEEE Access
Multidisciplinary | Rapid Review | Open Access Journal

Received February 5, 2020, accepted February 25, 2020, date of publication March 2, 2020, date of current version March 16, 2020.

Digital Object Identifier 10.1109/ACCESS.2020.2977347

Enhancement of Spectral Efficiency and Power Budget in WDN-PON Employing LDPC-Coded Probabilistic Shaping PAM8

LIN ZHOU[1,2], HAILIAN HE[1], YAMEI ZHANG[1], YIFAN CHEN[2], QINGHUA XIAO[2], AND ZE DONG[1,2], (Member, IEEE)

[1]Xiamen Key Laboratory of Mobile Multimedia Communications, College of Information Science and Engineering, Huaqiao University, Xiamen 361021, China
[2]Fujian Key Laboratory of Light Propagation and Transformation, College of Information Science and Engineering, Huaqiao University, Xiamen 361021, China

Corresponding author: Ze Dong (zdong9@hqu.edu.cn)

This work was supported in part by the Natural Science Foundation of China under Grant 61401166 and 61302095, in part by the Fujian Province Science Fund for Distinguished Young Scholars under Grant 2016J06015, and in part by the Quanzhou City Science and Technology Program of China under Grant 2018C108R and 2018C116R.

ABSTRACT A 5 × 60 Gb/s low-density parity-check (LDPC) coded WDM-PON using 8-level pulse amplitude modulation (PAM8) signals with probabilistic shaping (PS) over 20-km standard single-mode fiber (SSMF) with direct detection is proposed and experimentally demonstrated. Each optical carrier at the optical line terminal (OLT) carries a 20-Gbaud probabilistically-shaped LDPC-coded PS-PAM8 signal from a conventional uniform PAM16 signal following a designed approximate Gaussian distribution (AGD). A LDPC-based bit-interleaved coded modulation scheme with iterative decoding (BICM-ID) is utilized to recover the inherently overlapped symbols due to the proposed PS mapping. Combining decision-directed least-mean-squares (DD-LMS) and constant modulus algorithm (CMA), a blind feedback pre-equalizer is adopted to reduce the frequency loss of the signal owing to imperfect electro-optical components in experiment. As for experimental verification and application, 1.48-dB superior receiver power sensitivity and 1.7-dB launch fiber power optimization are gained respectively by using LDPC-coded PS-PAM8 signals in WDM-PON, which can bring higher spectral efficiency and power loss budget for the optical distribution networks.

INDEX TERMS WDM-PON, probabilistic shaping, PAM8, BICM-ID, LDPC, loss budget, pre-equalization.

I. INTRODUCTION

Wavelength division multiplexing passive optical network (WDM-PON) with large bandwidth and low latency is a hopeful technique to meet the needs for large channel rate in future heterogeneous access networks [1], [2]. Lots of techniques have been deeply studied to achieve higher data rate and spectral efficiency (SE) [3]. Optical coherent detection in WDM-PON possessing prominent receiver power sensitivity (RPS) has the capability of providing adequate system loss budget for the optical distribution networks (ODNs). However, high complexity of coherent receiver in every practical optical network unit (ONU) will be an important issue in commercial application [4]. As a highly developed modulation format with low cost and simplified calculating complexity for next generation high-speed interconnection, 4/8-level pulse amplitude modulation (PAM4/8) signals are widely used in 200G/400G interface of optical signal transmission with direct detection [5]–[7]. Based on these superiorities, it is believed that the PAM modulation is a prospective candidate for future WDM-PON. However, if more ONUs are to be used, it is challenging for such networks adopting PAM modulations to obtain superior system loss budget, due to the electro-optical devices with limited bandwidth and fiber nonlinear effect [8].

By employing probabilistic shaping (PS) mapping, the optical access networks based on PAM modulation can offer better RPS and higher SE due to its reduced average transmitted energy, which is carried out by transmitting lower-power modulated symbols with higher probability [9]–[12]. Moreover, it is beneficial for a WDM-PON to significantly reduce average transmitted power of PS-PAM signal, which are able to weaken the system's fiber nonlinear effect [12]. As a result, the increased launch power is able

The associate editor coordinating the review of this manuscript and approving it for publication was Qunbi Zhuge.

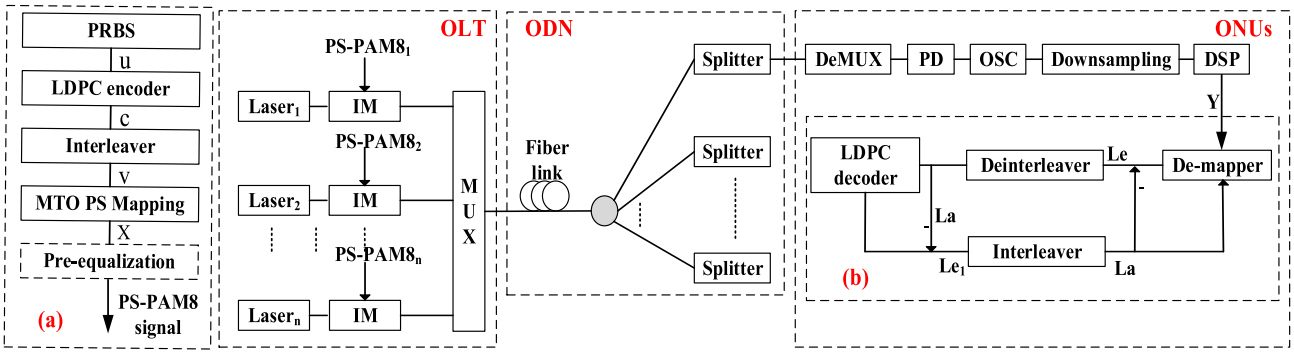

FIGURE 1. Principle for the WDM-PON employing LDPC-coded PS-PAM8, (a): LDPC-coded PS-PAM8 signal generation based on MTO mapping, (b) jointly iterative decoding based on LDPC-coded BICM-ID system.

to be shared for the requirement of loss budget. Compared with conventional PAM, more ONUs can thus be able to decode signals when employing PS-PAM, and the aggregate capacity in the optical splitter-based networks can thereby increase.

Trellis shaping was proposed in [13] and it was further studied in [14, Chap. 4] and [15, Sec. 4.4]. Designed shaping codes are necessary to select the symbols with low energy for transmission. So it is not easy to adapt various shaping rates. Shell mapping [16] was another method to obtain shaping gain. However, efficiently indexing the shells is a difficult work. In [17], shaping code was employed in bit-interleaved coded modulation (BICM) system, in which a one-to-one shaping code was proposed. Nevertheless, only limited gains are acquired. In [18], [19, Chap. 7], Böcherer proposed a novel shaping scheme, in which the uniformly distributed symbols of the source were firstly transformed into non-uniformly distributed symbols. Secondly, the probabilistically shaped symbols were encoded by FEC encoder. However, in this scheme, shaping was accomplished over several consecutive transmission blocks, which may result in higher latency and error propagation over successive blocks at the receiver.

In this work, we first introduce a PS-PAM8 approach based on many-to-one (MTO) mapping by reshaping 16-pulse into 8-pulse amplitude modulated signal obeying the designed approximate Gaussian distribution (AGD) into a WDM-PON system with the advantages of improved power loss budget and spectral efficiency. The proposed shaping technique does not require extra shaping code, which can achieve lower transmission rate loss and lower implementation complexity compared with that of conventional methods.

In the following sections, the proposed LDPC-coded PS-PAM8 scheme based on MTO mapping cooperated with BICM with iterative decoding (BICM-ID) is given a detailed presentation. At the receiver of the proposed scheme, decoding of the overlapped symbols caused by many-to-one mapping is a challenging task, which needs the powerful error correcting capability of channel code. In the experiment, a 5 $\times$ 60 Gb/s WDM-PON adopting LDPC-coded PS-PAM8 with direct detection is presented and experimentally verified. The optical line terminal (OLT) consists of 5 optical carriers, each of them carrying a 20-Gbaud probabilistically shaped LDPC-coded PS-PAM8 signal reshaped from a standard PAM16 signal. The inherently overlapped symbols in PS mapping, assigned in a well-designed binary LDPC code, are identified out by soft-decision based jointly iterative decoding in the LDPC-coded BICM-ID system. Based on the experimental verification, the proposed WDM-PON system employing PS-PAM8 can acquire the RPS improvement of 1.48 dB and the fiber nonlinear effect tolerance enhancement of 1.7 dB over a 20-km standard single-mode fiber (SSMF) channel. Consequently, the proposed system is expected to offer more sufficient loss budget for the legacy ODNs.

II. THE PRINCIPLE FOR THE LDPC-CODED PS-PAM8 WDM-PON

The block diagram of the proposed WDM-PON adopting PS-PAM8 with LDPC coding is displayed in Fig. 1. The lightwave emitted from the continuous lightwave (CW) laser is modulated via intensity modulators (IMs), which are driven by downstream LDPC-coded PS-PAM8 signal. The generation element of the driving signal is illustrated as Fig. 1(a). The binary source (pseudo random binary sequence, PRBS) is denoted as $\mathbf{u}$ with a length of K, then the source stream is linearly encoded via a LDPC encoder with the rate of R $=$ K/N. After the encoder, the output codeword $\mathbf{c}$ is permuted by an interleaver to produce the interlaced sequence $\mathbf{v}$. The PS mapper processes sequence $\mathbf{v}$ with probabilistic shaping technique to generate $\mathbf{X}$ as mapped PS-PAM8 symbols. For PS implementation, each mapped symbol is united by $(m+1)$ bits, hence the length of $\mathbf{X}$ is $\mathrm{N}/(m+1)$, where $m = \log_2(\mathrm{M})$ and M is the order of the proposed PS-PAM signal. Moreover, in the proposed PS mapping scheme, more than one labels are able to mapped onto one same constellation point, generating unequal probabilities of modulated symbol transmission. Similarly, the optical PS-PAM8 signals are unequally generated for WDM transmission. After multiplexing by an optical multiplexer (MUX), the downstream signals will be delivered to the remote terminal (RT) in the splitter-based ODN. Then the downstream signals are orderly routed and directly detected at the ONU afterwards. There exists a direct receiver at the ONU comprised of an

analog-to-digital converter (ADC) and a photo-detector (PD). The analog LDPC-coded PS-PAM8 signal passes through the PD for optical-to-electrical conversion and the ADC for digitalization in series. For each ONU, the digital signal is processed by down-sampling with two samples per symbol and digital signal processing (DSP). It is noted that PS-PAM8 signal based on MTO mapping as downstream data is of good compatibility with upstream data in other typical PON architecture [20].

The LDPC decoding part is shown in Fig. 1(b). The deliberate superimposed symbols in PS-PAM8 mapping are discerned by BICM-ID system with joint iterative soft-decision decoding algorithms. After DSP, the retrieved PS-PAM signals, denoted as vector **Y,** is firstly processed to provide the *a priori information* for received bits. Then the LDPC-based BICM-ID system is employed for both de-mapping and decoding. The main frame of the BICM-ID system at the receiver is the combination of a PS de-mapper and a LDPC decoder, which is carried out by adopting soft-input soft-output (SISO) decoding and concatenated with the suitable de-interleaver and interleaver. The reliability of each bit, calculated by the de-mapper or decoder, is described as *log-likelihood ratios* (LLRs) which are the log probability of '0' divided by probability of '1'. La represents the *a priori information* of de-mapper, and Le denotes the output *extrinsic information* of de-mapper.

1) PS de-mapper: The *Euclidean distance* between ideal PS-PAM8 symbol and every actual received symbol is calculated, and then the symbol-based reliability is computed with the aid of input *a priori information* $La(v_j)$. The value of LLR for every bit is obtained by the *maximum a posteriori* (MAP) algorithm. Then, Le, the *extrinsic information* for each bit, is able to be calculated by

$$Le(v_j) = \log(\frac{P(v_j = 0|Y, La(v_j))}{P(v_j = 1|Y, La(v_j))}) - La(v_j) \tag{1}$$

2) LDPC decoder: The *extrinsic information* stream of the de-mapper is de-interleaved and sent into the decoder as the *a priori information*. It is well-known that a LDPC decoder can be regarded as connection of a variable-node decoder (VND) and a check-node decoder (CND) in series. After inner iterations between VND and CND, the LDPC decoder output eliminates the corresponding *a priori information* to acquire *extrinsic information* $\mathbf{Le}_1$, where $\mathbf{Le}_1 = \mathbf{LLR} - \mathbf{La}$. After the interleaver, the *extrinsic information* is delivered to the de-mapper as *a priori information* for de-mapping. This process is named outer iteration. In short, the de-mapper and LDPC decoder will jointly keep working as a pair of SISO decoders till the maximum outer iteration number is met.

A. INFORMATION RATE

Let X be the source information, Y denotes the received information, and then *mutual information* (MI) I(X; Y) can be represented by a multivariate function of r variables $\{p(x_1), p(x_1), \mathrm{L}, p(x_r)\}$, where $p(x)$ is the probability distribution of the input information and $\sum p(x_i) = 1$ [21]. According to the principle of Shannon information theory, MI can be defined as

$$\begin{aligned}
\mathrm{I}(\mathbf{X};\mathbf{Y}) &= \sum_{x\in\mathbf{X}}\sum_{y\in\mathbf{Y}} p(x,y)\log\frac{p(x,y)}{p(x)p(y)} \\
&= \sum_{x} p(x)(\sum_{y} p(y|x)\log p(y|x)) \\
&\quad - \sum_{y}\log p(y)(\sum_{x} p(x,y)) \\
&= -\sum_{x} p(x)H(\mathbf{Y}|\mathbf{X}=x) - \sum_{y}\log p(y)p(y) \\
&= \mathrm{H}(\mathbf{Y}) - \mathrm{H}(\mathbf{Y}|\mathbf{X}) = \mathrm{H}(\mathbf{X}+\mathbf{N}) - \mathrm{H}(\mathbf{N})
\end{aligned} \tag{2}$$

where $p(y|x)$ is the channel transition probability function, and $\mathrm{H}(g)$ is the function of information entropy. Reliable communication is feasible if the transmission rate per real dimension does not overstep the channel capacity

$$C = \max_{\{\mathrm{p(x)}\}} \mathrm{I}(\mathbf{X};\mathbf{Y}) \tag{3}$$

According to Equation-2, the entropy of X should be maximized to approach the channel capacity. In this paper, the input distribution of modulated symbols should follow the designed AGD to be close to the channel capacity.

B. OPTIMIZED MANY-TO-ONE MAPPING SCHEMES

Recently, most existing PS schemes in WDM-PON are designed by constant composition distribution matching (CCDM) [22]. For the PS encoder in CCDM, all the output bit stream is invariably restrained within the edges of the corresponding input bit stream. For instance, there are totally 20 binary possibilities obeying Bernoulli (1/2) distribution in CCDM-based PS-PAM8. Nevertheless, only 8 out of 20 possible binary combinations are chosen as the distributer output. Thus by fixed-to-fixed mapping, the input symbols, "000", "001", "010", "011", "100", "101", "110" and "111", are correspondingly converted into the output symbols, "000111", "001101", "010011", "011001", "100011", "101001", "110010" and "111000", which results in another 3 bits ($3/6 = 50\%$) to be overheads. In the same way, in the PS-PAM8 case, the redundancy ratio of 33.3% (2/6) can be foreseeable for probabilistic shaping. In addition, it is also necessary to transmit error-correction codes in fiber-optic communication systems, which brings overheads as well. Reference [9] proposed a probabilistic amplitude shaping (PAS) scheme to make the PS match the FEC system by using a single superfluous bit which could share the redundancy for both LDPC code and PS mapper. Nevertheless, there still exists the defect of high redundancy in this sort of system because double overheads are unavoidable in CCDM and FEC. Different from conventional PS schemes by redundant overheads addition, the proposed PS scheme by Gallager many-to-one mapping in this paper can effectively promote the communication efficiency due to the absence of PS overheads. Reference [10] made use of turbo code and many-to-one mapping for the PS-QAM scheme.

Although a novel joint probabilistic and geometric shaping was proposed and realized with CAP signal based PON in [23] to prominently cut down the launch fiber power at the optical line terminal (OLT), the hardware complexity of CAP signal will be much higher than PAM besides the higher hardware demand for geometric shaping. Reference [24] proposed a new multi-level constellation compression modulation (MCCM) to reduce the number of constellation points and it was confirmed in GFDM-PON system. However, the employed CAP modulation format requires a much more complicated DSP compared with the PAM8 modulation in our scheme. Unlike the direct-detected 1-dimention PAM signal, the complex QAM signal requires coherent detection or CAP modulation. Although the QAM-DMT signal can be direct-detected, the high cost and complexity is less suitable for PON.

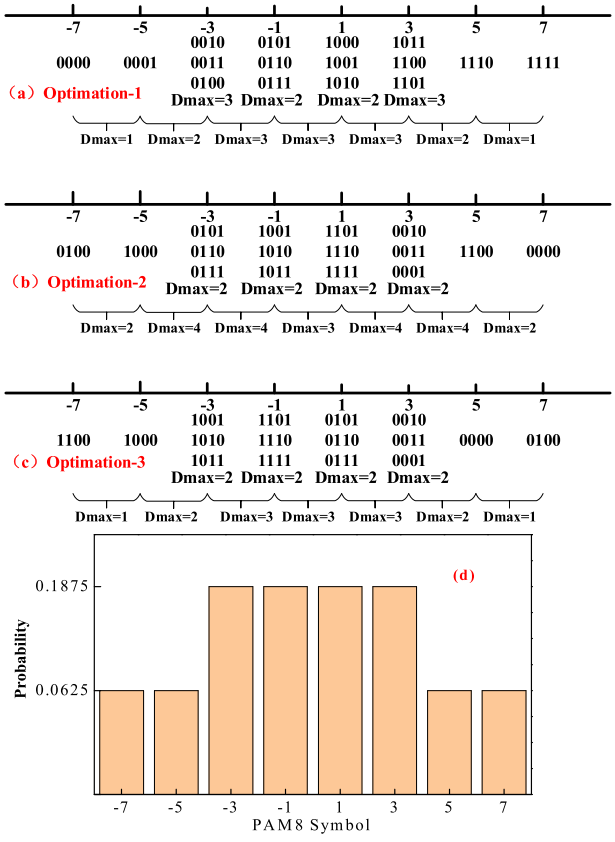

FIGURE 2. MTO mapping schemes for PS-PAM8, (a): Optimation-1, (b) Optimation-2, (b) Optimation-3, and (d) The probability distribution of Optimation-3.

Reshaped from 4-bit symbols, the proposed many-to-one PS-PAM8 with 8 pulse levels is shown in Fig. 2, in which all of 16 symbols are mapped into 8 points. The probability mass function (PMF) for each symbol is inherent. For the proposed PS-PAM8, three overlapped symbols are mapped into one same signal point on the innermost points of PAM8. As a result, each point of the four innermost ring is transmitted with the probability of 3/16, the MI is $2+2\times(1-(1/3\log 3+2/3\log 3/2)) = 2.16$ bits/symbol. Similarly, each point in outermost ring is transmitted with the probability of 1/16, respectively. Evidently, the MI is 4 bits/symbol. Assuming the codeword length is infinite, there exists a code with the rate of less than $(1/4\times 4+3/4\times 2.16)/4 = 0.65$, which can achieve arbitrarily low BER, if the probability distribution of transmitted symbols could be optimized.

For example, PS-PAM8 with 8 points can be mapped from 4-bit symbols, i.e., a total of 16 symbols can be mapped into 8 points. The many-to-one mapping law for PS-PAM8 is shown as Fig. 2(a). It follows the AGD without the optimization of symbols hamming distance. The scheme with Optimation-2 not only follows AGD, but also minimizes hamming distance between overlapped symbols as shown in Fig. 2(b). For the Optimal mappings, both the minimum hamming distances between overlapped symbols, and that between adjacent symbols are optimized, as shown in Fig. 2(c), i.e. optimation-3. Obviously, their maximum Hamming distances are significantly reduced by optimization. The probability distribution by MTO mapping based on optimation-3 is correspondingly shown as inserted Fig. 2(d).

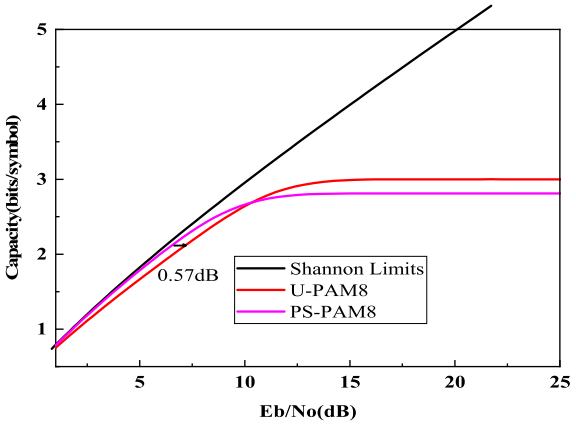

FIGURE 3. Capacity of coded modulation system with different modulation formats.

Figure 3 demonstrates the channel capacity of conventional uniform PAM8 and the proposed PS-PAM8, respectively. Obviously, in the low SNR region, the performance of our proposed PS-PAM8 can be improved to approach to the Shannon capacity. Theoretically, about 0.57-dB shaping gain can be acquired for the proposed PS-PAM8 compared with the conventional uniform one.

C. EXIT

In the preceding subsection, optimized many-to-one PS-PAM8 mapping scheme is provided. In this subsection, in order to further demonstrate the effectiveness of the proposed PS-PAM8 signal, extrinsic information transfer (EXIT) chart is used to theoretically analyze the LDPC-coded BICM-ID system [25]. At the receiver in Fig. 1(b), the SISO de-mapper extracts a priori information from the received sequence, and computes the posteriori information for the LDPC decoder. Besides the internal iteration between the VND and CND, the information exchange also performs between the de-mapper and the LDPC decoder. The EXIT chart comparison

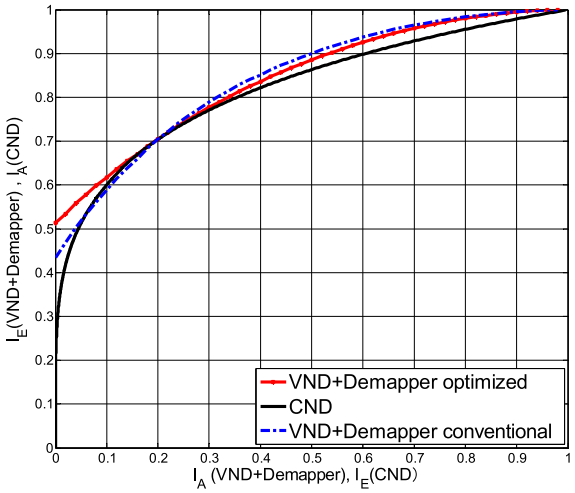

FIGURE 4. EXIT chart analysis for PS-PAM8, Eb/No = 7.9 dB.

for the proposed PS-PAM8 and the unshaped one is displayed in Fig. 4. As well as we know, when the VND-de-mapper curve and the CND curve in the chart are just close but do not intersect, the capacity of the corresponding mapping can be obtained. In fact, there is a very narrow passageway between the optimized curves in the chart. Oppositely, the conventional curves intersect each other, which leads to inevitable performance loss. One can also see from Fig. 4 that the optimized threshold of proposed PS scheme is confirmed.

III. EXPERIMENTAL SETUP

The experimental setup for 5 × 60 Gb/s WDM-PON system with LDPC-coded PS-PAM8 based on MTO mapping is shown in Fig. 5. An 18-GHz-bandwidth arbitrary waveform generator with 40 GSa/s sampling rate is used to generate the 20 Gbaud LDPC-coded PS-PAM8 signal. Five 50 GHz channel spaced external cavity lasers (ECLs) are utilized to generate 5 optical carriers. After two 45 GHz electrical amplifiers (EAs), two electrical PS-PAM8 signals are utilized to modulate the even and odd WDM channels via two 40GHz Mach-Zehnder modulators (MZMs). To couple and flatten different channels, a programmable wavelength selective switch (WSS) is subsequently used after 2 polarization maintenance optical couplers (PM-OCs).

For frequency loss because of the key photoelectric devices at the OLT, such as DAC, EAs, and MZMs, a 20-Gbaud standard PAM8 signal is transmitted as a reference signal in optical back-to-back (BTB) link to compute the transport function by the reversed FIR response based on cascaded constant modulus algorithm (CMA) and decision-directed least-mean-squares (DD-LMS), which is used to pre-equalize the PS-PAM8 signal [26].

To illustrate the performance of pre-equalization, the eye diagrams for both the proposed PS-PAM8 and the standard unshaped PAM8 exhibited in Fig. 5(a)-(d), respectively. Obviously, the PS-PAM8 signals are with better eye opening compared with the standard ones. Both of the signals with pre-equalization display much clearer profile than the ones without pre-equalization.

After transmission over 20-km SSMF ($g = 1.3\ (W \cdot km)^{-1}$ and $D = 17$ ps/nm/km) via the ODN, the LDPC-coded PS-PAM8 signal is chosen by a tunable 23-GHz optical filter. One variable optical attenuator (ATT) and one EDFA are employed to evaluate BER. At the ONU, the optical-to-electrical conversion of the proposed optical signal is carried out by a 40 GHz PD. Then a 50 GSa/s sampling rate digital oscilloscope is utilized to implement the A/D conversion and data acquisition. Then the proposed 20-Gbaud electrical signal is sent into the DSP module. The received data are processed by off-line DSP. Primarily, the received digital signal is operated by down-sampling with two samples per symbol. Secondly, two 13-tap and adaptive T/2-spaced FIR filters based on CMA, are utilized to preliminarily retrieve the 8-order coefficients of the PS-PAM8 signal [27].

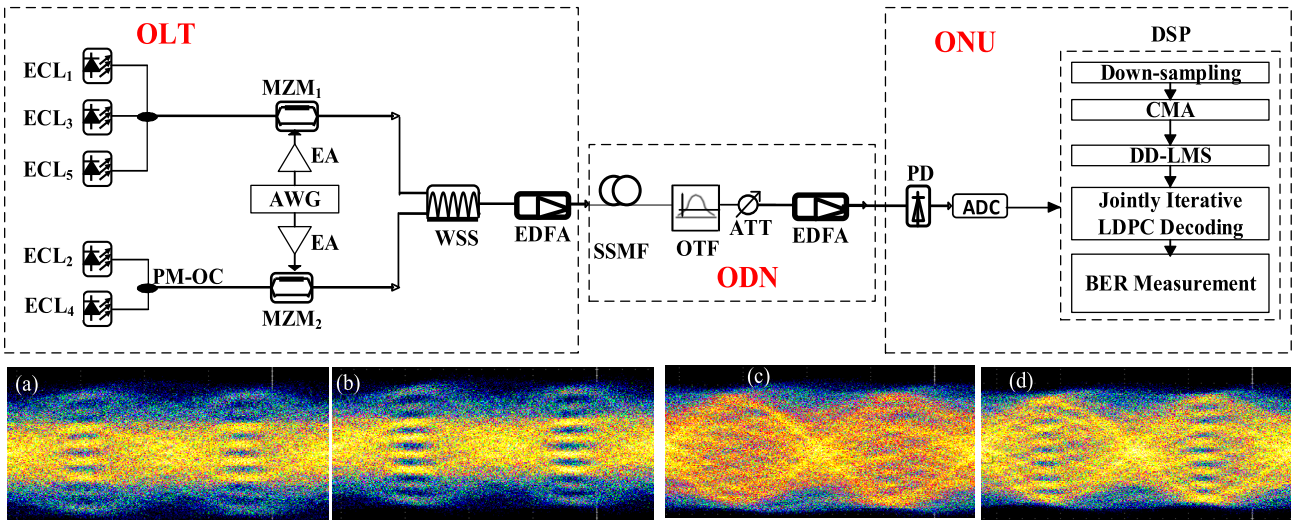

FIGURE 5. Experimental setup for 5 × 60 Gb/s WDM-PON based on LDPC-coded PS-PAM8. Eye diagram (in optical BTB link), (a) and (b): PS-PAM8 signal without and with pre-equalization, respectively, (c) and (d): standard PAM8 signal without and with pre-equalization, respectively.

Furthermore, the DD-LMS digital FIR filter is applied to process an accurate convergence with the eight-level decision [28], [29]. Finally, the recovered symbols of PS-PAM8 signal are softly decided and decoded by LDPC-based FEC.

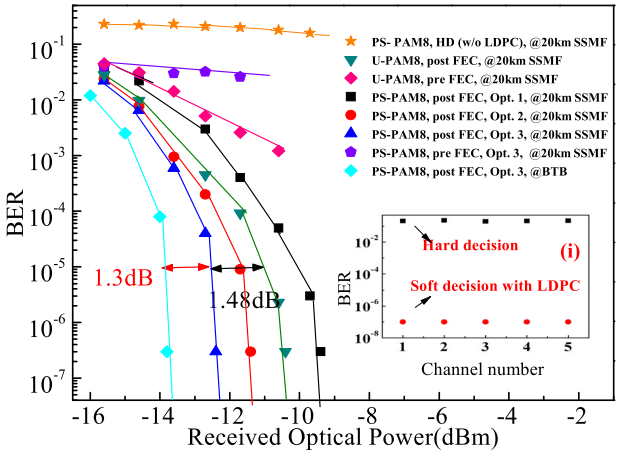

FIGURE 6. BER versus received optical power over 20-km SSMF transmission. Inset (i): BER performance for all 5 channels after 20-km SMF (received power = −13dBm), Opt.: optimization, U-PAM8: uniform PAM8.

IV. EXPERIMENTAL RESULTS

Figure 6 shows the BER performance for 20-Gbaud PS-PAM8 WDM-PON signals. In the experiment, the total number of source bits is 3000000. For comparison, the PS-PAM8 signal without LDPC coding (orange star curve) is simply demodulated by hard decision. On the contrary, after the first iterative loop between the de-mapper and decoder, one can see a BER gap for the PS-PAM8 signal by only hard decision (orange star) and pre-FEC (violet pentagon). The overlap caused by the proposed MTO mapping can never be revised by hard decision only, which results in the phenomenon of error floor around 1.5×10^{-1}. Furthermore, if the soft-decision de-mapper works alone without the joint iteration (violet pentagon curve, pre-FEC PS-PAM8), there still remains ambiguity. But in contrast to hard decision case, the BER performance can still be improved. When the joint iteration (soft-decision) of PS de-mapper and LDPC decoder is adopted, the conspicuous improvement of the BER from 1.5×10^{-1} to 3×10^{-7} can be acquired. Compared with the standard PAM8, the maximal shaping gain obtained by the optimization-3 mapping scheme for the PS-PAM8 signal over 20-km SSMF is 1.48 dB at the BER of 1×10^{5}, with the help of LDPC coding. Without the proposed optimization, the BER performance is even worse than that of standard PAM8 with LDPC coding. This is because the confusion and errors of the overlapped symbols are much easier to occur without the optimization. In the optical BTB link, for the proposed PS-PAM8, at the BER of 1×10^{-5}, the necessary received power is −13.82 dBm. There exists 1.30-dB power loss over 20-km SSMF transmission because of the chromatic dispersion and fiber nonlinear effect. The experimental BER curves after the five 20-km WDM transmission are shown in Fig. 6(i).

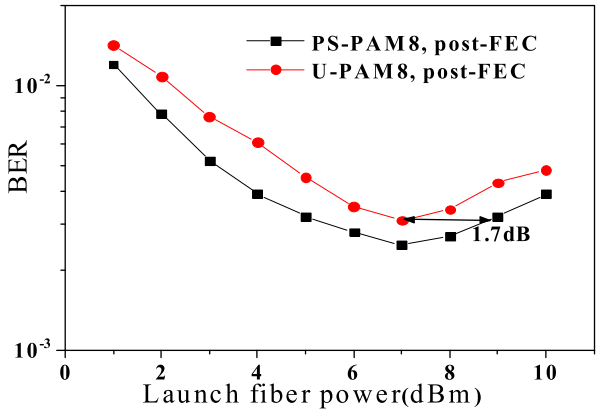

FIGURE 7. BER versus launch fiber power over 20-km SSMF transmission (received power = −15dBm).

In Figure 7, the performance of PS-PAM8 WDM-PON signal (received power = −15 dBm) versus different launch fiber power is shown. The BER for standard PAM8 and PS-PAM8 (both launch power = 2 dBm) are 1.08×10^{-2} and 7.8×10^{-3}, respectively. One can see that if the launch power enlarges to 7 dBm, the BER for standard PAM8 signal and that for PS-PAM8 signal are decreasing to 3.1×10^{-3} and 2.5×10^{-3}, respectively. The tolerance to fiber nonlinear effect by high launch fiber power for PS-PAM8 is superior to that for U-PAM8 because of the reduced average transmitted power by the proposed probabilistic shaping technique. At the BER of 2.5×10^{-3}, 1.7-dB fiber nonlinear effect tolerance improvement is obtained for the PS-PAM8 WDM-PON signal compared with the system based on standard PAM8.

V. CONCLUSION

A 5 × 60-Gb/s LDPC-coded WDM-PON using PS-PAM8 over 20-km SSMF is proposed and experimentally demonstrated. Without any shaping code, each optical carrier carries a 20-Gbaud probabilistically shaped PS-PAM8 signal from a 4-bit U-PAM16 signal. The probability mass function of signal symbols follows the approximate Gaussian distribution. And the maximum Hamming distances of both overlapped symbols and adjacent symbols are optimized. Then, a rate-1/2 binary LDPC code is adopted to enhance the reliability of the PS-PAM8. The inherently overlapped symbols caused by PS mapping are de-mapped and retrieved by the joint soft decoding algorithms. Compared with the unshaped U-PAM8, the proposed system with direct detection exhibits enhanced fiber nonlinear effect tolerance and superior optical receiver sensitivity. Consequently, ampler system loss budget for the legacy optical distribution networks is gained.

REFERENCES

[1] A. Shahpari, J. D. Reis, R. Ferreira, D. M. Neves, M. Lima, and A. Teixeira, "Terabit+ (192 × 10 Gb/s) Nyquist shaped UDWDM coherent PON with upstream and downstream over a 12.8 nm band," in *Proc. OFC*, 2013, pp. 1–3, Paper PDP5B.3.

[2] J. Zhang, J. Yu, F. Li, N. Chi, Z. Dong, and X. Li, "11 × 5 × 9.3 Gb/s WDM-CAP-PON based on optical single-side band multi-level multi-band carrier-less amplitude and phase modulation with direct detection," *Opt. Express*, vol. 21, no. 16, pp. 18842–18848, Aug. 2013.

[3] G. Bosco, A. Carena, V. Curri, P. Poggiolini, and F. Forghieri, "Performance limits of Nyquist-WDM and CO-OFDM in high-speed PM-QPSK systems," *IEEE Photon. Technol. Lett.*, vol. 22, no. 15, pp. 1129–1131, Aug. 1, 2010.
[4] Z. Dong, H.-C. Chien, J. Yu, J. Zhang, L. Cheng, and G.-K. Chang, "Very-high-throughput coherent ultradense WDM-PON based on Nyquist-ISB modulation," *IEEE Photon. Technol. Lett.*, vol. 27, no. 7, pp. 763–766, Apr. 1, 2015.
[5] K. Zhong, X. Zhou, T. Gui, L. Tao, Y. Gao, W. Chen, J. Man, L. Zeng, A. P. T. Lau, and C. Lu, "Experimental study of PAM-4, CAP-16, and DMT for 100 Gb/s short reach optical transmission systems," *Opt. Express*, vol. 23, no. 2, p. 1176, Jan. 2015.
[6] N. Eiselt, J. Wei, H. Griesser, A. Dochhan, M. Eiselt, J.-P. Elbers, J. J. V. Olmos, and I. T. Monroy, "First real-time 400G PAM-4 demonstration for inter-data center transmission over 100 km of SSMF at 1550 nm," in *Proc. OFC*, 2016, pp. 1–3, Paper W1K5.
[7] N. Eiselt, J. Wei, H. Griesser, A. Dochhan, M. H. Eiselt, J.-P. Elbers, J. J. V. Olmos, and I. T. Monroy, "Evaluation of real-time 8 × 56.25 Gb/s (400G) PAM-4 for inter-data center application over 80 km of SSMF at 1550 nm," *J. Lightw. Technol.*, vol. 35, no. 4, pp. 955–962, Feb. 15, 2017.
[8] R. van der Linden, N. C. Tran, E. Tangdiongga, and A. M. J. Koonen, "Improvement on received optical power based flexible modulation in a PON by the use of non-uniform PAM," in *Proc. Eur. Conf. Opt. Commun. (ECOC)*, Sep. 2017, pp. 1–3.
[9] G. Bocherer, F. Steiner, and P. Schulte, "Bandwidth efficient and rate-matched low-density parity-check coded modulation," *IEEE Trans. Commun.*, vol. 63, no. 12, pp. 4651–4665, Dec. 2015.
[10] M. P. Yankov, D. Zibar, K. J. Larsen, L. P. B. Christensen, and S. Forchhammer, "Constellation shaping for fiber-optic channels with QAM and high spectral efficiency," *IEEE Photon. Technol. Lett.*, vol. 26, no. 23, pp. 2407–2410, Dec. 1, 2014.
[11] W. Idler, F. Buchali, L. Schmalen, E. Lach, R.-P. Braun, G. Bocherer, P. Schulte, and F. Steiner, "Field trial of a 1 Tb/s super-channel network using probabilistically shaped constellations," *J. Lightw. Technol.*, vol. 35, no. 8, pp. 1399–1406, Apr. 15, 2017.
[12] K. Wang, X. Li, M. Kong, P. Gou, W. Zhou, and J. Yu, "Probabilistically shaped 16QAM signal transmission in a photonics-aided wireless terahertz-wave system," in *Proc. OFC*, 2018, pp. 1–3, Paper M4J.7.
[13] D. Forney, "Trellis shaping," *IEEE Trans. Inf. Theory*, vol. 38, no. 2, pp. 281–300, Mar. 1992.
[14] S. A. Tretter, *Constellation Shaping, Nonlinear Precoding, and Trellis Coding for Voiceband Telephone Channel Modems: With Emphasis on ITU-T Recommendation V.34*. Norwell, MA, USA: Kluwer, 2002.
[15] R. F. H. Fischer, *Precoding and Signal Shaping for Digital Transmission*. Hoboken, NJ, USA: Wiley, 2002.
[16] A. K. Khandani and P. Kabal, "Shaping multidimensional signal spaces. I. optimum shaping, shell mapping," *IEEE Trans. Inf. Theory*, vol. 39, no. 6, pp. 1799–1808, Nov. 1993.
[17] S. Y. Le Goff, B. S. Sharif, and S. A. Jimaa, "Bit-interleaved turbo-coded modulation using shaping coding," *IEEE Commun. Lett.*, vol. 9, no. 3, pp. 246–248, Mar. 2005.
[18] G. Bocherer and R. Mathar, "Operating LDPC codes with zero shaping gap," in *Proc. IEEE Inf. Theory Workshop*, Oct. 2011, pp. 330–334.
[19] G. Böcherer, "Capacity-achieving probabilistic shaping for noisy and noiseless channels," Ph.D. dissertation, RWTH Aachen Univ., Aachen, Germany, 2012.
[20] C. Pan and F. R. Kschischang, "Probabilistic 16-QAM shaping in WDM systems," *J. Lightw. Technol.*, vol. 34, no. 18, pp. 4285–4292, Sep. 15, 2016.
[21] A. Kraskov, H. Stögbauer, and R. G. Andrzejak, "Hierarchical clustering based on mutual information," *Europhys. Lett.*, vol. 70, no. 2, pp. 278–284, 2005.
[22] P. Schulte and G. Bocherer, "Constant composition distribution matching," *IEEE Trans. Inf. Theory*, vol. 62, no. 1, pp. 430–434, Jan. 2016.
[23] X. Xu, B. Liu, X. Wu, L. Zhang, Y. Mao, J. Ren, Y. Zhang, L. Jiang, and X. Xin, "A robust probabilistic shaping PON based on symbol-level labeling and rhombus-shaped modulation," *Opt. Express*, vol. 26, no. 20, pp. 26576–26589, Sep. 2018.
[24] L. Jiang, B. Liu, Y. Mao, X. Wu, J. Ren, X. Xu, S. Han, J. Zhao, L. Zhao, T. Sun, and L. Zhang, "A novel multi-level constellation compression modulation for GFDM-PON," *IEEE Photon. J.*, vol. 11, no. 2, pp. 1–11, Apr. 2019.
[25] L. Zhou, W. Huang, S. Peng, Y. Chen and, and Y. He, "An improved design of Gallager mapping for LDPC-coded BICM-ID system," *Electron. J.*, vol. 20, no. 1, pp. 16–21, 2016.
[26] S. J. Savory, "Digital filters for coherent optical receivers," *Opt. Express*, vol. 16, no. 2, pp. 804–817, 2008.
[27] Z. Dong, J. Yu, H.-C. Chien, N. Chi, L. Chen, and G.-K. Chang, "Ultra-dense WDM-PON delivering carrier-centralized nyquist-WDM uplink with digital coherent detection," *Opt. Express*, vol. 19, no. 12, pp. 11100–11105, May 2011.
[28] A. J. Viterbi and A. M. Viterbi, "Nonlinear estimation of PSK-modulated carrier phase with application to burst digital transmission," *IEEE Trans. Inf. Theory*, vol. IT-29, no. 4, pp. 543–551, Jul. 1983.
[29] X. Zhou and J. Yu, "Multi-level, multi-dimensional coding for high-speed and high-spectral-efficiency optical transmission," *J. Lightw. Technol.*, vol. 27, no. 16, pp. 3641–3653, Aug. 15, 2009.

LIN ZHOU received the B.E., M.E., and Ph.D. degrees in information and communications engineering from Xidian University, Xi'an, China, in 2004, 2007, and 2011, respectively. He is currently an Associate Professor with the College of Information Science and Engineering, National Huaqiao University, Xiamen, China. His research interests include LDPC codes, polar codes, capacity-approaching coded modulation systems, wireless communications, and optical communications.

HAILIAN HE received the bachelor's degree in electronic information and technology from Hunan Normal University, China, in 2006, and the master's degree in circuits and systems from Hangzhou Dianzi University, China, in 2009. Her research interest includes high-data rate optical communication systems.

YAMEI ZHANG received the B.E. degree in communications engineering from the Central South University of Forestry and Technology, Changsha, Hunan, China, in 2018. She is currently pursuing the M.E. degree in electronics and communications engineering with Huaqiao University, Xiamen, Fujian, China. Her research interests include LDPC codes, wireless communications, and optical communications.

YIFAN CHEN received the B.E. degree in communication engineering from the Hunan University of Science and Technology, Xiangtan, Hunan, China, in 2015. He is currently pursuing the M.E. degree in electronics and communication engineering with Huaqiao University, Xiamen, Fujian, China. His main research interest includes fiber-optic communication.

QINGHUA XIAO received the B.S. degree in optical information science and technology from the Changsha University of Science and Technology, Changsha, Hunan, in 2016. She is currently pursuing the M.S. degree in optical engineering with Huaqiao University, Xiamen, Fujian. Her research interest includes optical-fiber communication.

ZE DONG (Member, IEEE) received the joint Ph.D. degree from the Georgia Institute of Technology, USA, and Hunan University, China, in 2011. He worked as a Research Fellow with the Georgia Institute of Technology, from 2011 to 2014. He is currently an Electrical Engineering Professor with the College of Information Science and Engineering, Huaqiao University, Xiamen, China. He was granted as The Top Young Talents of Fujian Province and the Fujian Province Science Fund for Distinguished Young Scholars. He holds ten U.S. and five CN patents. He has published over 150 articles in prestigious journals and conference proceedings in the field of coherent optical coherent transmission systems, passive optical networks, and broadband radio-over-fiber systems.